

SELECTED RESULTS OBTAINED AT SYOWA STATION,
ANTARCTICA, BY RECEPTION OF KYOKKO
AND ISIS SATELLITE DATA

Takesi NAGATA, Takeo HIRASAWA, Hiroshi FUKUNISHI, Natsuo SATO
National Institute of Polar Research, 9-10, Kaga 1-chome, Itabashi-ku, Tokyo 173

and

Takeo YOSHINO

University of Electro-Communications, 5-1, Chofugaoka 1-chome, Chofu 182

Abstract: Satellite data acquisition facilities for ISIS-1 and -2 and EXOS-A (Kyokko) were installed at Syowa Station in January 1976. The VLF wideband and topside sounder data measured on ISIS-1 and -2 have been received on the routine basis since April 1976. The total number of the ISIS-1 and -2 passes received at Syowa Station in the period from April 1976 to August 1979 are 476 and 654, respectively. The reception of telemetry signals from EXOS-A began in February 1978. The total number of the passes received in the period of February 1978–August 1979 is 427. From the VLF wideband data measured with these satellites, emission regions of VLF hiss and saucer have been investigated. It is found that the hiss emission region with occurrence probability larger than 50% is located at 75°–85° geomagnetic latitude between 10 h and 14 h MLT on the dayside, and at 65°–80° geomagnetic latitude between 20 h and 02 h MLT on the nightside, while the saucer emission region with occurrence probability larger than 30% is located at 75°–85° between 10 h and 18 h MLT on the dayside and at 60°–70° between 18 h and 02 h MLT on the nightside. It is suggested that the hiss and saucer emission regions are closely associated with field-aligned currents.

1. Introduction

Satellite data acquisition facilities were built up at Syowa Station, Antarctica in January 1976, and the telemetry reception of the ISIS-1 and -2 data have been carried out on a routine basis since April 1976. As shown in Table 1, telemetry signals from 476 passes of ISIS-1 and 654 passes of ISIS-2 were received at Syowa Station in the period from April 1976 to August 1979. The reception of telemetry signals from the Japanese polar-orbiting satellite, EXOS-A (Kyokko) began at Syowa Station in February 1978. The total number of the EXOS-A passes received at Syowa Station during the period of February 1978–August 1979 is 427 (*cf.* Table 1). In the present paper, the obtained results of some of these satellite receptions will

Table 1. Monthly number of ISIS-1 and -2 satellite passes received at Syowa Station.

	1976		1977		1978			1979		
	ISIS-1	ISIS-2	ISIS-1	ISIS-2	ISIS-1	ISIS-2	EXOS-A	ISIS-1	ISIS-2	EXOS-A
January			24	23	18	13		0	2	
February			33	20	7	3	63	5	3	1
March			10	8	8	11	12	9	10	25
April	3	5	9	8	10	8	15	8	10	36
May	0	23	18	12	8	7	24	5	9	9
June	15	14	17	14	19	14	51	9	7	6
July	13	26	23	26	9	6	61	8	10	
August	26	21	11	6	9	10	55	8	7	10
September	23	38	8	13	6	11	10			
October	9	16	9	9	7	5	26			
November	11	46	7	6	7	7	23			
December	22	41	15	13	10	5				
Total	122	230	184	158	118	208	340	(52) Before Aug.	(58) Before Aug.	(87) Before Aug.

Selected Results Obtained by Kyokko and ISIS Satellites

be briefly summarized.

2. VLF Hiss and Saucer Emissions Measured by ISIS-1, -2 and EXOS-A

It is known that VLF hiss and saucer emissions are typical whistler mode waves observed in the VLF and LF range. VLF hiss is characterized by a broadband spectral structure (GURNETT, 1966), while VLF saucer is characterized by a hyperbolic shape in the frequency-time display (JAMES, 1976). These emissions were frequently observed by VLF wide-band receivers on board ISIS-1, -2 and EXOS-A. The apogee and perigee altitudes of ISIS-1 are 3526 km and 578 km, and the orbit inclination is 88.4° , while ISIS-2 is in a circular orbit of approximately 1400 km with an orbit inclination of 88.1° . The EXOS-A satellite was launched on February 4, 1978. The apogee and perigee altitudes are 3984 km and 638 km, and the orbit inclination is 65.3° .

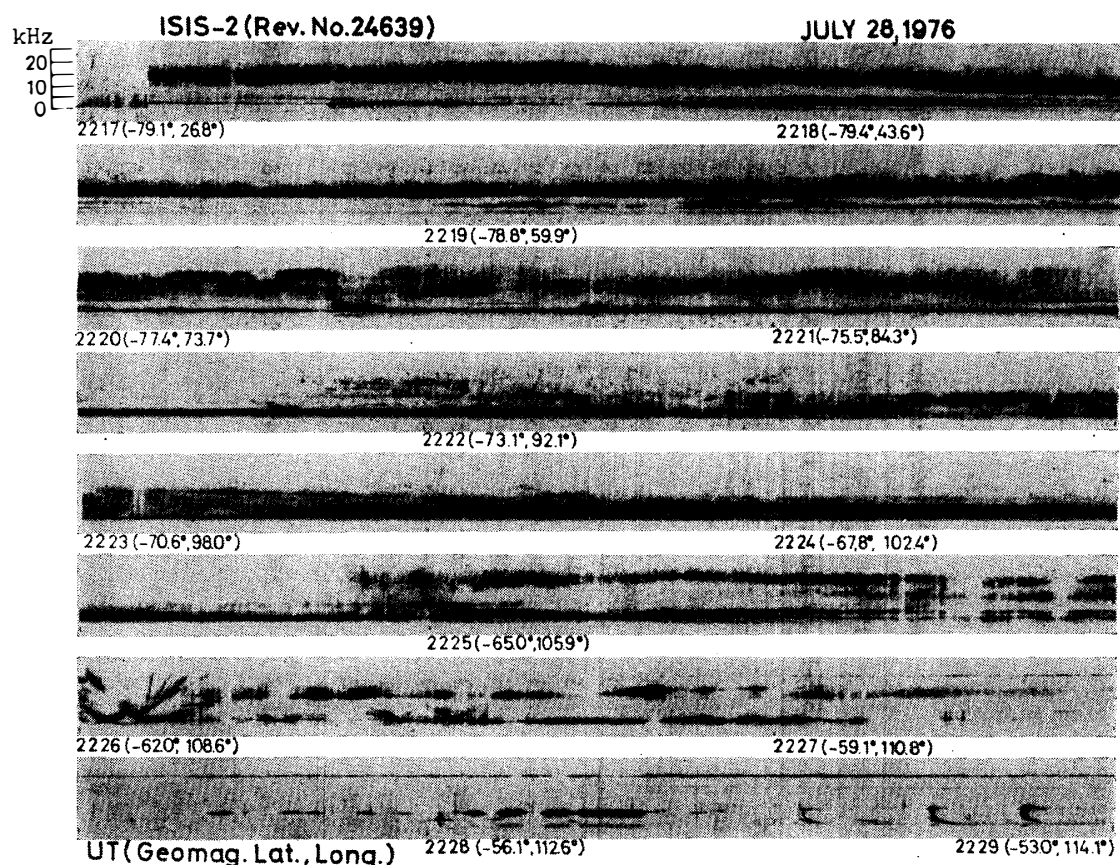


Fig. 1. Typical example of the ISIS-2 VLF spectrum showing a successive occurrences of VLF hiss, saucer and whistler as the satellite moved from high latitude to low latitude in the evening sector.

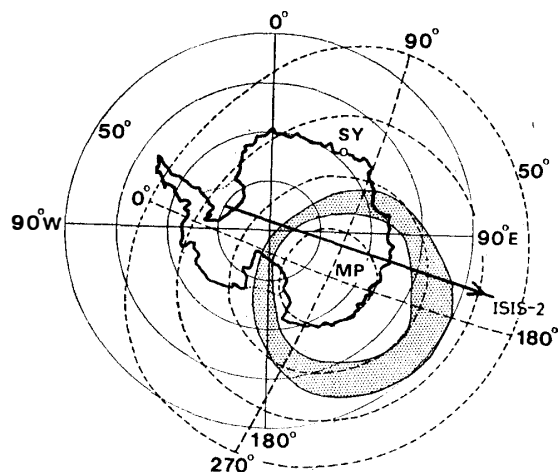


Fig. 4. Ground track of the ISIS-2 pass during the VLF emission event shown in Fig. 2 and its relation to the auroral oval given by FELDSTEIN (1963).

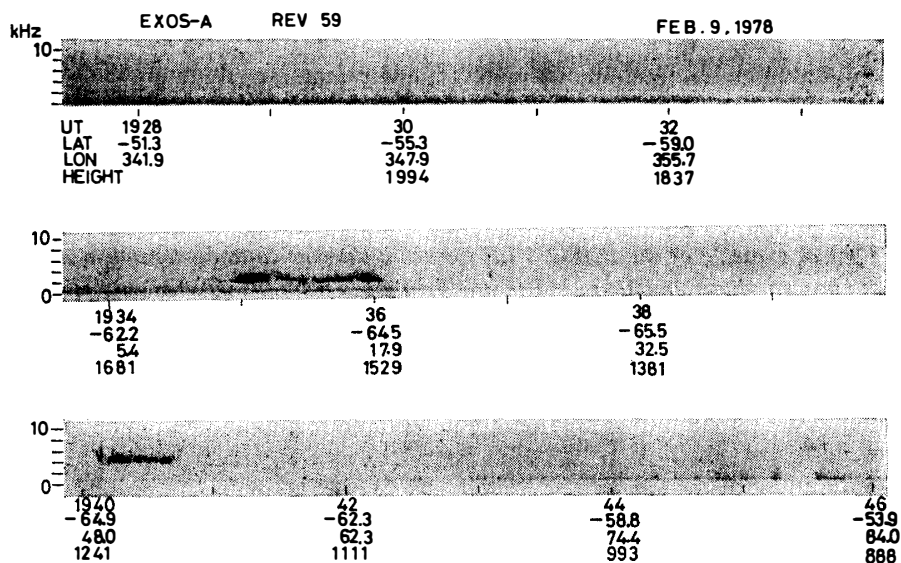


Fig. 5. Example of VLF emissions measured on EXOS-A (Kyokko) in austral summer. The ground track of EXOS-A in this example is given in Fig. 3.

Typical examples of VLF emissions measured with ISIS-2 in the austral winter are shown in Figs. 1 and 2. The ground tracks of ISIS-2 during these two periods, and their relationships to the auroral oval given by FELDSTEIN (1963), are illustrated in Figs. 3 and 4, respectively. These figures are useful for studying the relationship of the VLF hiss and saucer emission region to the auroral emission region, although the real auroral emission region may be different from the auroral oval obtained statistically by FELDSTEIN (1963). The magnitudes of K_p index during the obser-

vation periods of ISIS-2 presented in Figs. 1 and 2 were 2_+ and 3_- , respectively.

In the case shown in Figs. 1 and 3, Syowa Station was located at about 22h MLT, and ISIS-2 moved along the auroral oval in the evening sector from high latitudes toward low latitudes. It was found that VLF hiss emissions occurred continuously during the passage through the auroral oval, and then VLF saucer emissions followed near the equatorward edge of the auroral oval.

In the case shown in Figs. 2 and 4, Syowa Station was located at about 15h MLT, and ISIS-2 passed from the dayside cusp region to through the polar cap the auroral oval on the nightside. It is shown that VLF saucer emissions occurred at 74° geomagnetic latitude on the dayside, and then the events were followed by hiss emissions occurring continuously up to 85° geomagnetic latitude. In the polar cap region, VLF emissions were seldom observed. However, intense hiss emissions occurred again when ISIS-2 reached the nightside auroral oval.

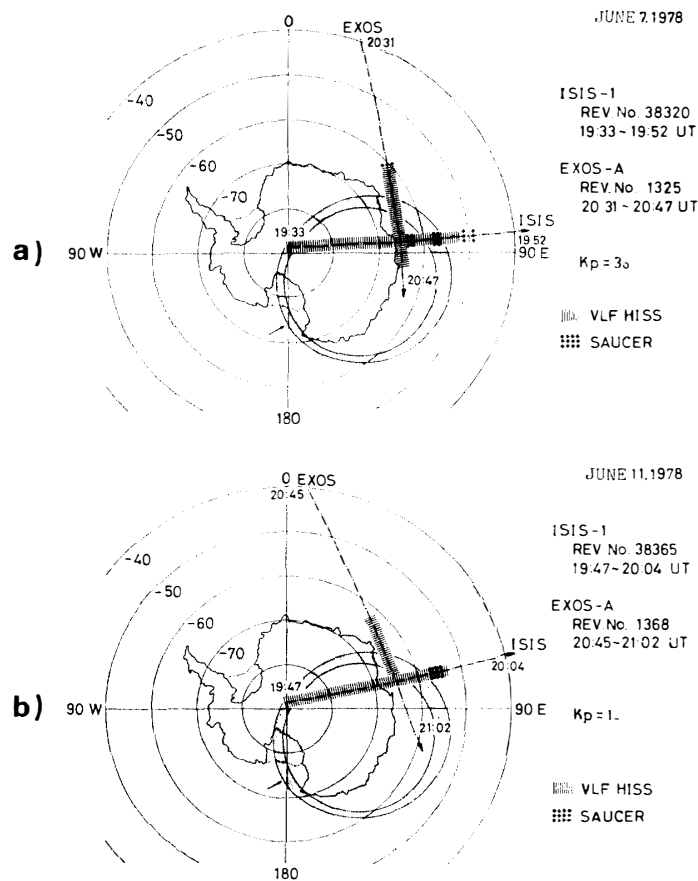


Fig. 6. Examples of coordinated observations of VLF hiss and saucer emissions with ISIS-1 and EXOS-A in the austral winter. The auroral oval given by FELDSTEIN (1963) is also illustrated in the figure. The arrow shows the magnetic local noon.

An example of VLF emissions observed on EXOS-A in the austral summer season is given in Fig. 5. The ground track of EXOS-A in this example is illustrated in Fig. 3. In general, the orbits of EXOS-A and the orbits of ISIS-1 and -2 cross at approximately right angle since the inclination of EXOS-A is 65.3° . As shown in Fig. 3, EXOS-A data are suitable for studying longitudinal extension of the VLF emission region in contrast with the ISIS-1 and -2 data which are suitable for studying the latitudinal extension. Therefore, coordinated observations of VLF emissions of EXOS-A and ISIS-1 and -2 can give both longitudinal and latitudinal ranges of the VLF emission region, if the orbits of both satellites intersect within a short time, of each other.

Examples of coordinated observations of EXOS-A and ISIS-1 during the austral winter season are presented in Fig. 6. We see in these figures that the emission region of VLF hiss is fairly wide in both longitude and latitude. It is also evident that the emission region of the VLF saucer is located adjacent to the equatorward edge of the hiss emission region.

3. Distribution of VLF Hiss and Saucer Emissions over the Southern Polar Region

VLF hiss and saucer emissions were selected from the frequency-time spectra of the 155 passes of ISIS-2 received at Syowa Station in 1976 and 1977. Then, the locations of the VLF hiss and saucer emission regions were plotted in geomagnetic latitude and local time coordinates. Fig. 7 shows the distribution of occurrence frequency of VLF hiss emissions in the austral winter season (April–September). The coverage of the ISIS-2 passes during these periods is shown in the polar plot given in Fig. 8. It can be seen that almost all local time regions are well covered, although the number of passes in the 20–02h MLT sector is fairly

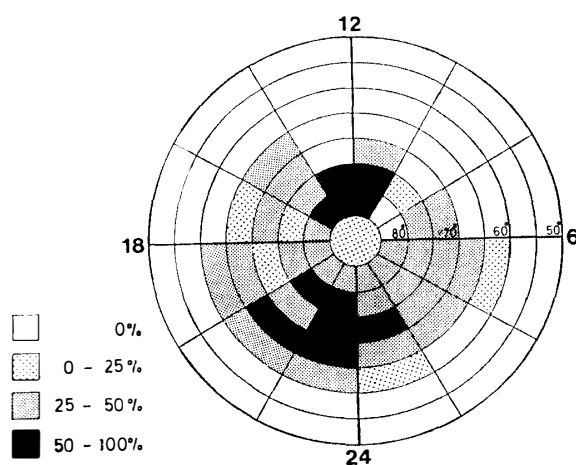


Fig. 7. Polar plot of VLF hiss occurrence percent in the geomagnetic latitude and local time coordinate (austral winter period, April–September).

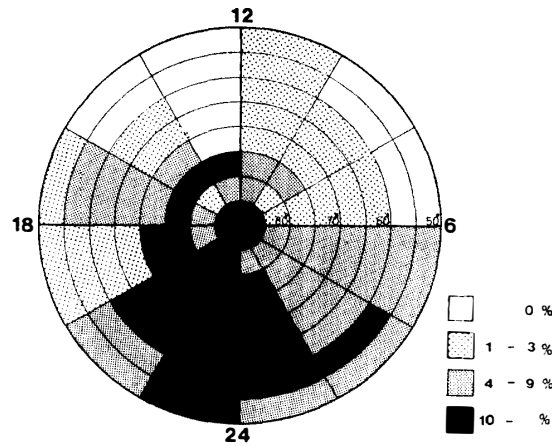


Fig. 8. Polar plot of ISIS-2 number of passes in the geomagnetic latitude and local time coordinates (austral winter period, April-September).

high compared with other local time regions.

From the polar plot of the VLF hiss occurrence frequency in Fig. 7, several tendencies can be found. They are:

- (1) Hiss emissions are not observed at latitudes lower than 60° geomagnetic latitude.
- (2) Hiss emissions are observed in all magnetic local time regions.
- (3) The hiss emission region on the dayside is located at 70° – 85° geomagnetic latitude with a symmetrical distribution about the noon-midnight meridian.
- (4) The hiss emission region on the nightside is located at 60° – 85° geomagnetic latitude with a high occurrence frequency at 65° – 80° and 20–02 h MLT.
- (5) The occurrence frequency of hiss emissions is quite low in the region above 85° around the geomagnetic pole.

The distribution of occurrence frequency of VLF saucer emissions is presented in Fig. 9, in which the occurrence frequency is plotted in geomagnetic latitude and local time coordinates. This polar plot shows following features.

- 1) The saucer emission regions with high occurrence probability are located both on the dayside and on the nightside just as are the emission regions of the VLF hiss.
- 2) The saucer emission region on the nightside is located at 55° – 80° geomagnetic latitude with a high occurrence frequency at 60° – 70° and 18–02h MLT.
- 3) The saucer emission region on the dayside is located at 75° – 85° geomagnetic latitude and 10–18h MLT.

The polar plot of occurrence frequency of VLF saucer emissions given in Fig. 9 shows the saucer emission region in the austral winter season, since saucer emissions were not observed at all on ISIS-2 in the austral summer season from

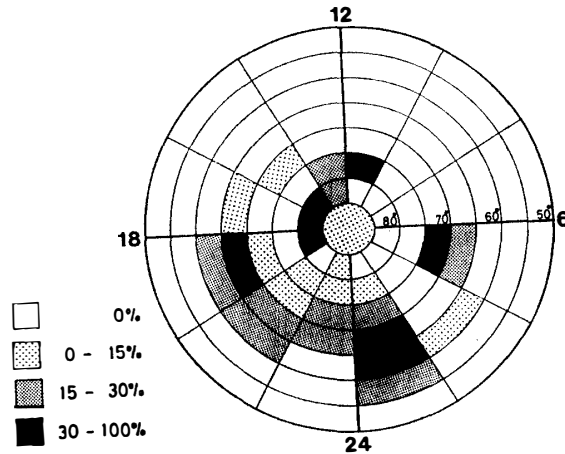


Fig. 9. Polar plot of VLF saucer occurrence percent in geomagnetic latitude and local time coordinates.

October to April. Fig. 10 shows the monthly number of the ISIS-2 passes with saucer events (hatched area) and the total monthly number of the ISIS-2 passes received at Syowa (unhatched area). A significant seasonal variation is found in the occurrence of VLF saucer emissions observed on ISIS-2. However, saucer emissions were observed on ISIS-1 in summer. This difference can be well explained by taking into consideration a change in altitude distributions of saucer emissions. The hatched area in Fig. 11 gives the number of passes as a function of altitude of ISIS-1 with saucer events while the unhatched area gives the total number of passes of ISIS-1 for (a) austral winter (April–September), and for (b) austral summer (October–March). Saucer emissions are observed at an altitude range of 500–4000 km with a maximum occurrence at 2500–3000 km in winter, while they

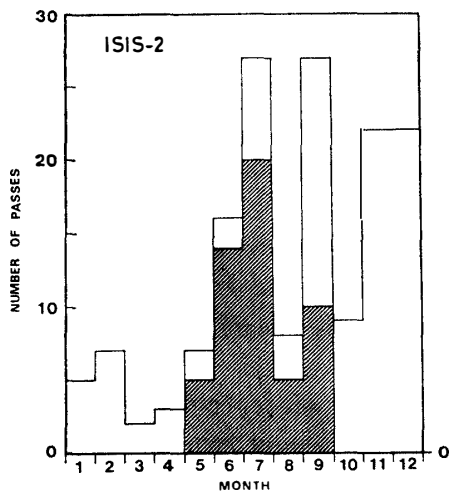
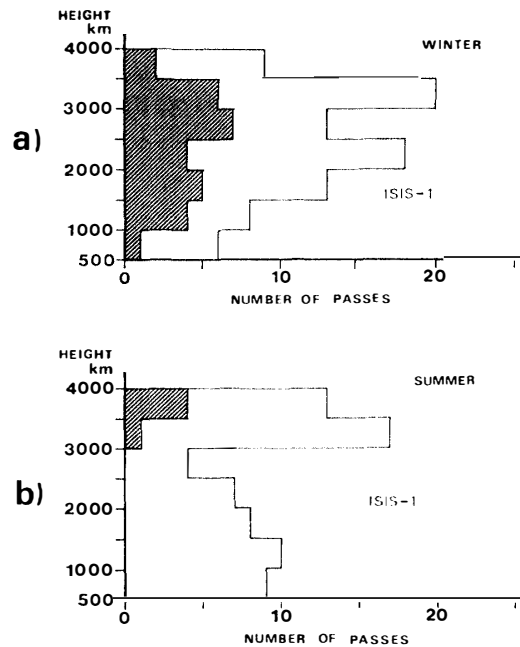


Fig. 10. Seasonal variation of occurrence of VLF saucer emissions. The unhatched histogram shows the total monthly number of passes of ISIS-2, while the hatched histogram shows the number of ISIS passes with saucer emissions.

Fig. 11. Altitude distribution of VLF saucer events. The un-hatched histogram indicates the total number of ISIS-1 passes used for data analysis, while the hatched area indicates the number of ISIS-1 passes with saucer emissions.

a) Austral winter period (April–September).

b) Austral summer period (October–March).



are observed only at altitudes higher than 3000 km in summer. Therefore, it is reasonable that saucer emissions can not be observed on ISIS-2 in summer since the ISIS-2 satellite is in a circular orbit near 1400 km in altitude.

4. Discussion

It has been shown both individually and statistically that the saucer emission region is located equatorward of the hiss emission region in the evening to midnight hours. It is found that a relationship between the hiss and saucer emission regions given in Figs. 7 and 9 is similar to the relationship between the upward and downward field aligned current regions presented by IJIMA and POTEMURA (1976). The result suggests that saucer emissions are generated by field-aligned currents downward toward the ionosphere, while hiss emissions are generated by upward field-aligned currents. Particularly, the existence of the saucer and hiss emission regions at 75° – 85° on the dayside strongly suggests that field-aligned currents in the dayside cusp region contribute to the generation of saucer and hiss emission.

The generation mechanism of saucer emissions is still unknown. However, a significant seasonal variation in the altitude distribution of saucer emissions given in Fig. 11 indicates that the electron density profile in the topside ionosphere is related to the growth rate of saucer emissions.

References

FELDSTEIN, Y. I. (1963): Some problems concerning the morphology of auroras and magnetic

disturbances at high altitudes. *Geomag. Aeron.*, **3**, 183–196.

GURNETT, D. A. (1966): A satellite study of VLF hiss. *J. Geophys. Res.*, **71**, 5599–5615.

IJIMA, T. and POTEMURA, T. A. (1976): Field-aligned currents in the dayside cusp observed by Triad. *J. Geophys. Res.*, **81**, 5971–5979.

JAMES, H. G. (1976): VLF saucers. *J. Geophys. Res.*, **81**, 501–513.

(Received April 30, 1980)